

RSC Advances



This is an *Accepted Manuscript*, which has been through the Royal Society of Chemistry peer review process and has been accepted for publication.

Accepted Manuscripts are published online shortly after acceptance, before technical editing, formatting and proof reading. Using this free service, authors can make their results available to the community, in citable form, before we publish the edited article. This *Accepted Manuscript* will be replaced by the edited, formatted and paginated article as soon as this is available.

You can find more information about *Accepted Manuscripts* in the [Information for Authors](#).

Please note that technical editing may introduce minor changes to the text and/or graphics, which may alter content. The journal's standard [Terms & Conditions](#) and the [Ethical guidelines](#) still apply. In no event shall the Royal Society of Chemistry be held responsible for any errors or omissions in this *Accepted Manuscript* or any consequences arising from the use of any information it contains.

Assistant effect of poly(methyl methacrylate) grafted carbon nanotubes on beta polymorph of poly(vinylidene fluoride) during microinjection

Feng Bai, Gang Chen, Min Nie*, Qi Wang

State Key Laboratory of Polymer Materials Engineering, Polymer Research Institute of Sichuan University, Chengdu 610065, China

Email: poly.nie@gmail.com

Fax: +86-28-85402465

Tel: +86-28-85405133

Abstract: Poly(vinylidene fluoride)(PVDF) with numerous electroactive beta crystals was achieved via melt-processing under the coupled effects of external flow field generated by microinjection and dipole-dipole interaction with poly(methyl methacrylate) grafted carbon nanotubes, which was significant for expanding the potential applications of piezoelectric PVDF devices.

Poly(vinylidene fluoride) (PVDF) is the best all-around electroactive polymer and exhibits great potential for application in sensors, ferroelectric memories and biomedical fields^{1, 2}. The unique electroactive properties strongly depend on its crystalline phases. PVDF possesses five polymorphs, among which α and β phases are the most investigated crystals. For α -PVDF, polymer chains are piled up in trans-gauche–trans-gauche(TGTG) conformation, where fluorine atoms normal to the chain are antiparallel and thus the dipoles neutralize each other, presenting non-polarization; on contrary, β -PVDF has an all-trans(TT) conformation with the dipoles fully aligned in the same direction and possesses the largest dipole moment and excellent piezo- and ferroelectric properties, i.e., electroactive of PVDF is associated with the content of polar β -PVDF³. However, α -PVDF is the most stable phase and is commonly obtained in normal melt-processing^{4, 5}. Therefore, high-level polar β -phase in PVDF materials is an on-going pursuit.

Up to now, many efforts have been devoted to the preferential formation of β -PVDF, such as mechanical stretching, solution crystallization in polar solvents, melt crystallization under high pressure and electrospinning. Moreover, incorporation of

nanofillers also has been proved to a facile route for enhancement of β -PVDF and suppression of α -PVDF^{6, 7}. Carbon nanotubes(CNTs) have zigzag carbon atoms, which match with TT conformation of β -PVDF so it is expected as ideal filler to induce crystallization of PVDF into β -phase⁸. But the energy of TT conformation of PVDF is higher than that of TGTG, and PVDF chains in the TGTG conformation easily are absorbed on the surface of pristine CNTs⁹. Direct addition of unmodified CNTs is failed for the increased β -PVDF. Recently, the interactions between local electric field and PVDF dipoles, such as hydrogen bond–dipole, ion–dipole, dipole–dipole, are found to facilitate the transformation from TGTG to TT conformation and thus chemical functionalized CNTs benefit the formation of β -PVDF¹⁰. Manna found that ester-functionalized CNTs promoted α - β transition by the special interaction of the $>C=O$ group and $>CF_2$ group of PVDF¹¹. Mandal prepared PMMA-functionalized CNTs via nitrene reaction and fabricated almost full β -PVDF through a solution mixing route¹². However, in the melt state, polymer chains interpenetrate and entangle each other, and the molecular motion is restricted compared to that in solution, depressing the transformation from TGTG to TT conformation. Therefore, high content of β -PVDF is not yet obtainable from the melt-cooled PVDF/functionalized CNTs composites even at high loading of the CNTs¹³ although melt processing is a facile and versatile processing way for preparation of smart devices like sensors and actuators.

It has been reported that external flow fields can get polymer chains

disentangled and induce coil-stretch transition, which is helpful for conversion of helix TGTG conformation to zigzag TT one^{14, 15}. Due to lower energy of TGTG conformation, the conversion is instable and the TT conformation easily relaxes via thermal motion. Expectantly, introduction of special interaction can retard the relaxation and stabilize TT conformation to promote the formation of β -PVDF^{4, 16}. In this study, poly(methyl methacrylate) (PMMA) firstly was grafted onto CNTs via solid-state mechanochemical process because there was the interaction between carbonyl groups of PMMA and PVDF and PVDF/PMMA blends were miscible in the molten state over the whole composition range^{17, 18}. Then, PMMA-g-CNTs/PVDF nanocomposites were mixed and microinjected, where very high shear rate ($>10^5\text{s}^{-1}$) was imposed on the polymer melts¹⁹. Utilizing the synergetic effects of the functionalized CNTs and external flow field, high-level β -PVDF was obtained directly through melt processing, providing a simple and efficient way to fabricate electroactive PVDF device. [Detailed description of materials, sample preparation and characterizations are provided in ESI]

Firstly, a self-designed pan-mill type equipment was adopted to achieve direct attachment of PMMA onto the surface of CNTs. This equipments exerted strong shearing force like a pair of three-dimensional scissors on the milling materials, bringing about solid mechanic-chemical reaction between polymer and filler²⁰. In this case, PMMA/CNTs mixtures(9/1) were fed into the solid-state mechanochemical equipment and the milled powders were extracted with boiling N,N-dimethylformamide(DMF) in Soxhlet extractor for 48h to remove free PMMA.

The obtained CNTs was named as PMMA-g-CNTs. According to our previous works²¹, PMMA underwent chain scission and formed free macroradicals during pan-milling processing. The radicals could be terminated at the surface of CNTs to allow the functionalization of CNTs with PMMA. [see FTIR spectra of PMMA-g-CNTs in ESI] The content of PMMA grafted onto CNTs was estimated based on the mass loss differences among the pure PMMA, CNTs and PMMA modified CNTs. As shown in Fig. 1, pristine CNTs showed no mass loss when heated to 600°C while pure PMMA was degraded completely. In comparison, PMMA-g-CNTs exhibited 18wt% weight-loss, suggesting PMMA was successfully grafted onto the CNTs surface. This was also confirmed by SEM photo in Fig. 1. Clearly, CNTs were wrapped by some polymer and the surface became uneven.

Subsequently, the compounding of PVDF and 0.5wt% pristine CNTs or PMMA-g-CNTs was conducted through DMF solution and the CNTs/PVDF nanocomposites were melt-processed on a Battenfeld MicroPower-5 molding machine (Wittmann Battenfeld GmbH, Austria). Since the introduced pristine CNTs and the functionalized CNTs were low (only 0.5%), the processing behaviors of PVDF remained unchanged. [Rheological results is described in ESI] For comparison, the static samples also were prepared under no stress filed, where the samples were melted at 190 °C in a hot stage for 5min followed by cooling. Since PVDF, CNTs/PVDF composite and PMMA-CNTs/PVDF composite prepared by static state and microinjection had similar crystallinity,

the relative amount of β -PVDF was key for preparation of electroactive PVDF device. [DSC results described in ESI] Figure 2 presented the conformation sensitive bands in the wavenumber range of 600 to 1500 cm^{-1} for the three samples prepared by static state and microinjection. The characteristic absorption peaks of α -PVDF with TGTG conformation appeared at 764, 796, 976 and 1218 cm^{-1} , while those at 840 and 1274 cm^{-1} were assigned to TT conformation of β -PVDF³. For the static samples in Fig. 2a, one can observe strong absorption peaks corresponding to α -PVDF and weak absorption ones representing β -PVDF. On the contrary, the characteristic absorption peaks of β -PVDF became visible under external flow field generated by microinjection and the intensities of β -PVDF overwhelmed that of α -PVDF with the presence of PMMA-g-CNTs, as shown in Fig. 2b. The relative amount of β -PVDF (F_{β}) was estimated according to the following equation:²²

$$F_{\beta} = \frac{X_{\beta}}{X_{\alpha} + X_{\beta}} = \frac{A_{\beta}}{1.26A_{\alpha} + A_{\beta}} \quad (1)$$

where X_{α} and X_{β} were mass fractions of α -PVDF and β -PVDF and A_{α} and A_{β} represented the absorbance intensities at 760 and 840 cm^{-1} , respectively. The calculated results were listed in Fig. 3. Clearly, there mainly existed α -PVDF via directly cooling from the polymer melts regardless of pristine CNTs and PMMA-g-CNTs, indicating that the two CNTs provided less help for the formation of β -PVDF at the static state. As to the microinjected pure PVDF and pristine CNTs/PVDF samples, it's observed that α -PVDF coexisted with β -PVDF and pristine CNTs slightly promoted the formation of β -PVDF. In a word, either CNTs or external flow field independently are ineffective enough to produce a large content of β -PVDF.

Very interesting, β -PVDF was dominant in PMMA-g-CNTs/PVDF nanocomposites prepared via microinjection and the fraction reached 95.1%, suggesting there were the cooperative effects of external force and PMMA-g-CNTs on the formation of β -PVDF. Since melt-processing is facile and versatile processing route to mould polymer objects, this study will expand the potential applications of piezoelectric PVDF devices.

Mechanism: α -form crystal with TGTG conformation, the most common polymorph, is frequently generated in the melt-cooled condition while β -PVDF having TT conformation is not always retained, since the free energy of the former conformation is lower than that of the later^{3,9}. The interaction between local electric field and PVDF dipoles is widely recognized as an accepted mechanism for the direct formation of β -PVDF²³: owing to the specific interaction, F atoms are located along one side of the PVDF chain, directly transforming molecular conformation into TT one and forming β -PVDF. In order to prepare high-level β -PVDF, PMMA with $>C=O$ group, which has a strong dipole-dipole interaction with $>CF_2$ groups of PVDF, was grafted onto the surface of CNTs via solid mechanic-chemical method. However, such interaction only works in the solution where PVDF chains spread out, which is favorable to the strong interaction between PVDF and PMMA-g-CNTs and the subsequent conversion of α - to β -PVDF²⁴. Different from β -PVDF in solution, entangled PVDF chains in the melt state are in the coil state and only few chains can be interacted with PMMA-g-CNTs²⁵, so the functionalized CNTs hardly affected the

formation of β -PVDF. Evidently, there is no shift of C–F stretching in the amorphous phase at 874cm^{-1} for the three PVDF samples prepared in the static state. Similar result also was manifested in other research²⁶. On the other hand, PVDF chains get stretched under high flow field, facilitating the transformation from helix TGTG conformation to zigzag TT conformation, but due to molecular thermal motion the stretched molecules are compelled to relax into TGTG conformation with low energy. As a result, numerous α -PVDF still existed in the microinjected pure PVDF sample. Pristine CNTs with zigzag carbon atoms, which match TT conformation of β -PVDF, could promote the formation of β -PVDF as the nucleating agent. But because the CNTs had little specific interaction with PVDF, the TT conformation relaxation was inevitable; and the absorbed energy of TT conformation on the surface of CNTs was higher than that of TGTG conformation. Therefore, it's clear that pristine CNT exerted positive effects on β -PVDF to a small extent. Upon PMMA's functionalization on CNTs, there were strong interactions between the $>\text{CF}_2$ groups of PVDF and the CNTs²⁷, as inferred from the shift of C–F stretching in the amorphous phase from 874cm^{-1} in pure PVDF to higher wavenumbers of 877cm^{-1} in PMMA-g-CNTs/PVDF nanocomposites(Fig. 2b). Obviously, the interaction could not only stabilize TT conformation generated during the microinjection, but also aid the conversion of TGTG into TT conformation. As a result, the formation of β -PVDF was significantly promoted under the synergistic effects of external flow field and PVDF-the functionalized CNTs interaction, and the microinjected PMMA-g-CNTs/PVDF nanocomposite was rich in β -form crystals.

In summary, high-level β -PVDF nanocomposites were fabricated successfully via microinjection at the help of PMMA-g-CNTs. The results showed that PVDF chains got stretched under high flow field during microinjection so the helix TGTG conformation was transformed into zigzag TT one. When PMMA-g-CNTs was incorporated into PVDF matrix, the special interaction between $>C=O$ group of PMMA and $>CF_2$ groups of PVDF stabilized TT conformation generated during the microinjection and further facilitated the conversion of TGTG conformation into TT conformation. Accordingly, almost full β -PVDF sample was obtained. Obviously, this melt-processing method for β -PVDF object is a step towards expanding the potential applications of piezoelectric PVDF devices.

This work is financed by the National Natural Science Foundation of China (51421061).

Notes and references

1. B. Chu, X. Zhou, K. Ren, B. Neese, M. Lin, Q. Wang, F. Bauer and Q. M. Zhang, *Science*, 2006, **313**, 334.
2. G. D. Kang and Y. M. Cao, *J Membrane Sci*, 2014, **463**, 145.
3. P. Martins, A. C. Lopes and S. Lanceros-Mendez, *Prog Polym Sci*, 2014, **39**, 683.
4. J. Yang, J. Wang, Q. Zhang, F. Chen, H. Deng, K. Wang and Q. Fu, *Polymer*, 2011, **52**, 4970.
5. M. Benz, W. B. Euler and O. J. Gregory, *Macromolecules*, 2002, **35**, 2682.

6. Y. Wu, S. L. Hsu, C. Honeker, D. J. Bravet and D. S. Williams, *J Phys Chem B*, 2012, **116**, 7379.
7. N. Jia, Q. Xing, G. Xia, J. Sun, R. Song and W. Huang, *Mater Lett*, 2015, **139**, 212.
8. S. Vidhate, J. Chung, V. Vaidyanathan and N. D'Souza, *Mater Lett*, 2009, **63**, 1771.
9. S. Yu, W. Zheng, W. Yu, Y. Zhang, Q. Jiang and Z. Zhao, *Macromolecules*, 2009, **42**, 8870.
10. G. Zhong, L. Zhang, R. Su, K. Wang, H. Fong and L. Zhu, *Polymer*, 2011, **52**, 2228.
11. S. Manna and A. K. Nandi, *J Phys Chem C*, 2007, **111**, 14670.
12. A. Mandal and A. K. Nandi, *J Mater Chem*, 2011, **21**, 15752.
13. G. H. Kim, S. M. Hong and Y. Seo, *Phys Chem Chem Phys*, 2009, **11**, 10506.
14. C. Xing, L. Zhao, J. You, W. Dong, X. Cao and Y. Li, *J Phys Chem B*, 2012, **116**, 8312.
15. Y. Ahn, J. Y. Lim, S. M. Hong, J. Lee, J. Ha, H. J. Choi and Y. Seo, *J Phys Chem C*, 2013, **117**, 11791.
16. Y. L. Liu, Y. Li, J. T. Xu and Z. Q. Fan, *ACS Appl Mater Inter*, 2010, **2**, 1759.
17. H. Sasaki, P. Kanti Bala, H. Yoshida and E. Ito, *Polymer*, 1995, **36**, 4805.
18. H. Song, S. Yang, S. Sun and H. Zhang, *Polym Plast Tech Eng*, 2013, **52**, 221.
19. A. L. Kelly, T. Gough, B. R. Whiteside and P. D. Coates, *J Appl Polym Sci*, 2009, **114**, 864.

20. W. Shao, Q. Wang, F. Wang and Y. Chen, *Carbon*, 2006, **44**, 2708.
21. H. Xia, Q. Wang, K. Li and G.-H. Hu, *J Appl Polym Sci*, 2004, **93**, 378.
22. B. Mohammadi, A. A. Yousefi and S. M. Bellah, *Polym Test*, 2007, **26**, 42.
23. A. Mandal and A. K. Nandi, *ACS Appl Mater Inter*, 2013, **5**, 747.
24. Y. Li, J. Z. Xu, L. Zhu, G. J. Zhong and Z. M. Li, *J Phys Chem B*, 2012, **116**, 14951.
25. R. Krishnamoorti, W. W. Graessley, A. Zirkel, D. Richter, N. Hadjichristidis, L. J. Fetters and D. J. Lohse, *J Polym Sci Part B: Polym Phys*, 2002, **40**, 1768.
26. K. Ke, P. Pötschke, D. Jehnichen, D. Fischer and B. Voit, *Polymer*, 2014, **55**, 611.
27. K. Zhang, J. Y. Lim and H. J. Choi, *Diam Relat Mater*, 2009, **18**, 316.

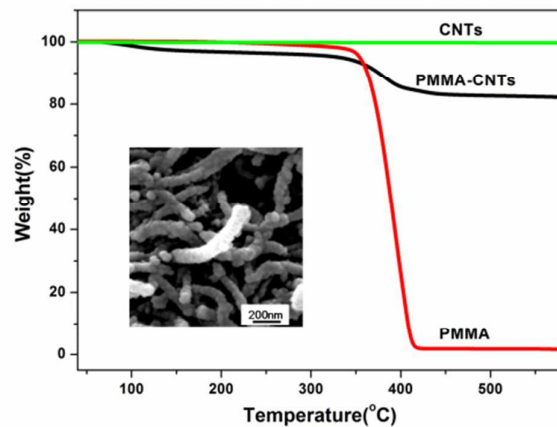


Figure 1 TGA weight loss curves for CNTs, PMMA and PMMA-g-CNTs via mechanic-chemical reaction. The insert shows SEM photo of PMMA-g-CNTs .

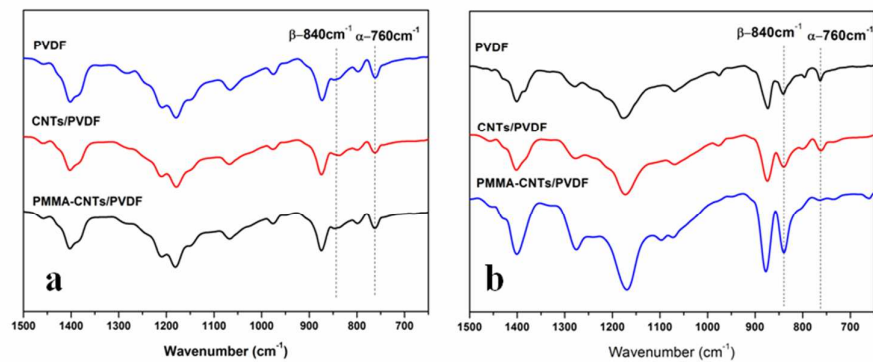


Figure 2 FTIR spectra of PVDF, CNTs/PVDF composite and PMMA-CNTs/PVDF composite prepared by static state (a) and microinjection(b)

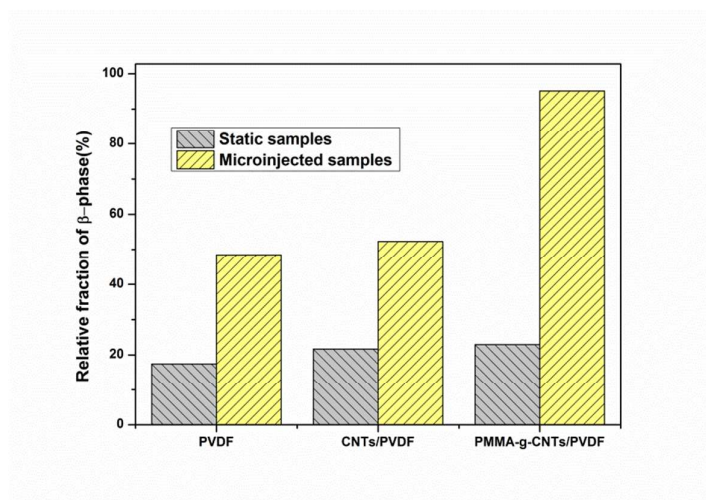


Figure 3 Relative fraction of β -phase in pure PVDF, CNTs/PVDF nanocomposite and PMMA-CNTs/PVDF nanocomposite prepared via static state and microinjection.